Chemical Synthesis and Characterization of Polyaniline Nanofiber Doped with Gadolinium Chloride

Shuling Zhang, Suqing Kan, Jinqing Kan

School of Chemistry and Chemical Engineering, Yangzhou University, Yangzhou 225002, People's Republic of China

Received 26 May 2005; accepted 30 August 2005
DOI 10.1002/app.23072
Published online 11 January 2006 in Wiley InterScience (www.interscience.wiley.com).

ABSTRACT: Gadolinium Chloride ($GdCl_3$) has been employed as dopant to synthesize conductive polyaniline (PANI) using chemical method. The resulting products were characterized using infrared spectroscopy, UV–vis spectra, scanning electron microscope, differential thermal analyzer, and X-ray diffraction. It was found that Gd^{3+} can interact with PANI chains and induce changes on the properties of PANI. The addition of $GdCl_3$ could greatly increase electrical conductivity and crystalline degree of PANI. Changes in UV–vis and FTIR spectra show that there exists interaction between gadolinium ions and PANI chain. The effect of different proportions of ammonium persulfate on the properties of PANI was also discussed. When the molar ratios of $GdCl_3$ to aniline is 2 : 1 and ammonium persulfate to aniline is 1 : 1, the more uniform and regular PANI nanofiber can be prepared. © 2006 Wiley Periodicals, Inc. J Appl Polym Sci 100: 946–953, 2006

Key words: polyaniline; gadolinium chloride; nanofiber; scanning electron microscope; X-ray diffraction; differential thermal analyzer

INTRODUCTION

Among all the conducting polymers, polyaniline (PANI) has attracted extensive attention because of its unique electrical, optical, and optoelectrical properties, as well as its ease of preparation and excellent environment stability.[1,2] Conducting polymers have long conjugated length and metal-like conductivity.[3] Many researchers have recently focused on its nanostructures possibly because of its promising applications in nanodevices, molecular electronics, microsensors, microactuators, and so on.[4–9]

The properties of PANI are strongly affected by a series of factors, for example, dopant, oxidant, and pH. Interactions of PANI with metal ions give rise to novel physical and chemical properties of the formed macromolecular complex.[10] Recently, it was reported that PANI could interact with many heavy metal ions[11–13] and rare-earth cations.[10,14,15] Because rare-earth elements have special electronic properties, *viz.* their f–f electronic transitions are relatively insensitive to perturbations in their chemical environment, complex formation of organic polymers with lanthanide ions is of particular interest. This aspect of rare-earth–polymer complexes is important in respect to their possible applications in the field of research and industrial applications (e.g., as emitting elements in organic light-emitting devices (OLEDs)[16–19] as well as dopant additions to enhance quantum yield in OLEDs,[20,21] and as catalysts for some polymer reactions.[14,22])

Nanostructure polymer can be prepared by some usual techniques, such as micro-emulsions, freeze-drying, atomizer spraying, and surface-spread film-patch methods,[23,24] which are inconvenient. Compared with these techniques, the chemical synthesis of conducting polymer is also of great importance since it is a very feasible route for the mass production.[25] Because the polymer cannot usually form a suitable ligand environment around the lanthanide ion,[10] lots of studies about the rare-earth–organic polymer complexes are needed. According to literature,[26] the existence of paramagnetic ions (for example, RE^{3+}) in solutions can greatly increase the effects of magnetic alignment and improve the properties of polymers. Cai et al.[15] investigated the effects of rare-earth cations on the preparation and properties of PANI obtained in magnetic field. Since the PANI can interact with many rare-earth cations, it is very interesting to chemically synthesize nanostructure PANI in the presence of $GdCl_3$.

In this study, we have tried to chemically synthesize PANI nanoparticles in the presence of $GdCl_3$. It was surprising to find that PANI nanofibers with the size of about 80 nm can be prepared in a solution containing $GdCl_3$. So, we mainly studied the effects of $GdCl_3$ on the nanoproperties of PANI; in addition, the effects of different proportions ammonium persulfate (APS) in the presence of $GdCl_3$ are also studied. Infrared

Correspondence to: J. Kan (jqkan@yzu.edu.cn).
Contract grant sponsor: National Science Foundation of China; contract grant number: 20273058.

spectroscopy (FTIR), UV–vis spectra, conductivity, X-ray diffraction (XRD), scanning electron microscope (SEM), and differential thermal analysis (DTA) are shown.

EXPERIMENTAL

The monomer aniline (reagent grade) was distilled into a colorless liquid under reduced pressure prior to use. APS and other chemicals were reagent grade and were used as received, without further pretreatment. $GdCl_3$ was of 99.9% purity. All of the aqueous solutions were prepared with double-distilled water.

PANI was synthesized in a solution containing 0.2 mol dm^{-3} aniline, 1.0 mol dm^{-3} hydrochloric acid (HCl), and different proportions of $GdCl_3$. APS of same molar ratio as aniline was slowly added into the solution in the rate of about 0.46 g min^{-1}, with stirring. PANI was also prepared in the presence of 0.4 mol dm^{-3} $GdCl_3$ by changing the APS content. The chemical polymerization of aniline was carried out at ambient temperature, ~10°C and the reaction time was 1 h. At the end of the reaction, the products were filtered, washed successively with 1.0 mol dm^{-3} HCl followed by ethanol until filtrate was colorless, and then dried at 75°C for 48 h.

The morphologies of PANI were observed using a scanning electron microscope (SEM XL-30 ESEM, Philips, Eindhoven, The Netherlands). The UV–vis electronic absorption spectra of all samples were obtained with UV-2550 spectrometer (Shimadzu, Kyoto, Japan) in the range of 300–900 nm. FTIR spectra of the samples were obtained with a FTIR spectrometer (Bruker, model Tensor 27, Germany). Pressed pellets of the powder samples ground with KBr were prepared for this purpose. DTA was performed using a differential thermal analyzer (Model CDR-4P, Shanghai, People's Republic of China), at a heating rate of 10°C min^{-1}, from 50 to 800°C. The conductivities of resulting products were measured at 20°C using conventional four-probe system. Dry powdered samples were made into pellets using a steel die 1.30 cm in diameter in a hydraulic press under a pressure of 7 tons, and the thickness of pressed pellets is 0.15 cm. WAXD patterns for the powder samples were taken on a M03XHF[22] diffractometer (Mac Science, Japan), using Cu Kα radiation (λ = 1.54056 Å), which were used to obtain the degree of crystallinity.

RESULTS AND DISCUSSION

Conductivity of resulting products

Table I gives the effects of $GdCl_3$ and APS concentration on the conductivity (σ) of resulting products. Samples 1–6 were synthesized chemically in 1.0 mol dm^{-3} HCl aqueous solutions containing 0.2 mol dm^{-3} aniline and different concentrations of $GdCl_3$, using 0.2 mol dm^{-3} APS as oxidant. Samples 1′–6′ were synthesized in 1.0 mol dm^{-3} HCl aqueous solutions containing 0.2 mol dm^{-3} aniline and 0.4 mol dm^{-3} $GdCl_3$, using different concentrations of APS as oxidant.

TABLE I
The Effects of Concentration of $GdC1_3$ and APS on Conductivity of Resulting Products

Sample	Gd^{3+} (mol dm^{-3})	APS (mol dm^{-3})	σ (S cm^{-1})
1	0		2.33
2	0.04		4.05
3	0.08		6.06
4	0.2		5.27
5	0.4		5.68
6	0.8		4.07
1′		0.05	1.21
2′		0.1	2.70
3′		0.2	5.68
4′		0.4	2.35
5′		0.8	$2.2l \times 10^{-3}$
6′		1.2	2.14×10^{-4}

By analyzing the conductivity values of samples 1–6, it can be seen clearly that the conductivity first increases with increasing $GdCl_3$ concentration, and when the concentration of Gd^{3+} is in the range of 0.08–0.4 mol dm^{-3}, the fluctuation in conductivities is not much. The conductivity is the highest when the concentration of Gd^{3+} is 0.08 mol dm^{-3}. These results reveal the effects of rare-earth cation on the conductivity, and that the gadolinium salt induces higher conductivity, which is comparable with that of control HCl-doped PANI. This may be because the added Gd^{3+} can interact with PANI chain[15]; they are trapped in the polymer chain or attach themselves loosely to the polymer backbone. Then polymer chains are formed more regularly, and electron transfer is increased along the chains, which results in an increase of conductivity. However, with further increase in Gd^{3+} concentration, the conductivities begin to decrease. It is because excessive Gd^{3+} affects the structure of PANI chain, which makes the conductivity of PANI decrease. This is consistent with the literature.[27]

As for the samples 1′–6′, when the concentration of APS is 0.2 mol dm^{-3}, namely, the molar ratio of APS to aniline is 1 : 1, the conductivity is maximum. When the molar ratios of APS to aniline are 4 : 1 and 6 : 1, the conductivities decreased rapidly, which is about 3–4 order of magnitude smaller than that of the PANI obtained with optimum amount of APS. This may be because the oxidative ability of APS is very strong. On one hand, it can oxidize aniline to free radical cation:

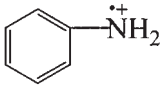

therefore, the polymerization happens on the mechanism of free radical; on the other hand, it can oxidize

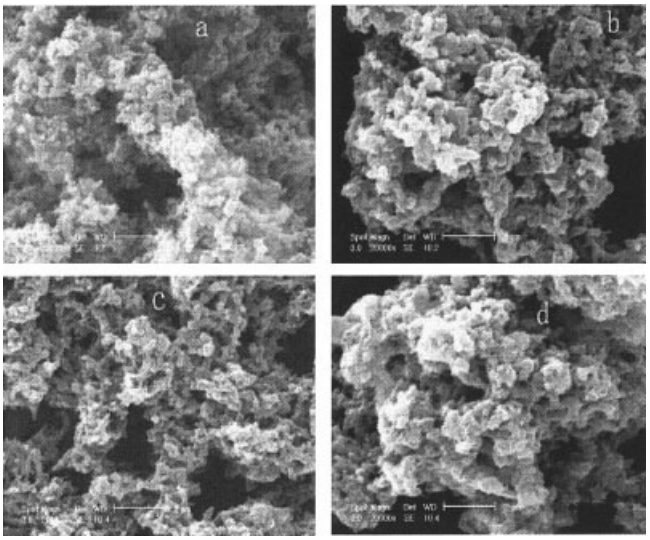

Figure 1 Effect of different proportions of Gd^{3+} on the morphology of PANI. The molar ratio of Gd^{3+} to aniline: (a) 0, (b) 1 : 1, (c) 2 : 1, and (d) 4 : 1.

aniline to other byproducts, which depends on the different reaction conditions.[28] When the molar ratio of APS to aniline is smaller, a small amount of APS was used up rapidly in the solution, and the aniline could not be oxidized completely. With the addition of excessive amounts of APS, it oxidized the different intermediate molecules and formed different products. Furthermore, because the PANI was peroxidized, some soluble small molecules were formed. So, the conductivities of samples 5′ and 6′ are smaller than that of the others.

Effects of different proportions $GdCl_3$ and APS on the morphology of PANI

Figure 1 shows SEM morphologies of PANI obtained in the solution containing 0.2 mol dm^{-3} aniline, 1.0 mol dm^{-3} HCl, and different concentrations of $GdCl_3$. It was found that the PANI particles are all between 80 and 200 nm as in Figures 1(a)–1(d). The PANI particles synthesized without Gd^{3+} tend to agglomerate together. When the $GdCl_3$ of same molar ratio as aniline was added into the solution, the PANI particles become distinct and uniform and with the increase in the $GdCl_3$ concentration, the PANI tend to form fiber-shaped morphology and are more distinct. However, when the molar ratio of $GdCl_3$ to aniline is 4 : 1, excessive Gd^{3+} makes PANI particles tend to agglomerate together and become very indistinct. That is to say, when the molar ratio of $GdCl_3$ to aniline is 1 : 1 or 2 : 1, it is more advantageous to chemically synthesize PANI nanofibers.

The results mentioned earlier show that the content of $GdCl_3$ can affect the morphology of chemically synthesized PANI. When $GdCl_3$ was added into the reaction solution, the Gd^{3+} was doped into the PANI chain and it may coordinate with PANI chain. The increase of $GdCl_3$ content in the solution improved the doping degree of PANI and promoted the diffusion of Gd^{3+} into the PANI chain leading to increase in the coordination of Gd^{3+} with PANI chain.[29] So, PANI particles become more and more distinct and uniform as the concentration of $GdCl_3$ increases. However, with further increase in $GdCl_3$ concentration, the aggregation of $GdCl_3$-doped PANI tends to occur (see Fig. 1(d)), which may be similar to the aggregation of micelles, and the morphology becomes very indistinct and the average size also increases. So, too much $GdCl_3$ is disadvantageous to obtain the more uniform and regular PANI nanofibers.

Figure 2 shows SEM morphologies of PANI obtained in the solution containing 0.2 mol dm^{-3} aniline, 1.0 mol dm^{-3} HCl, and 0.4 mol dm^{-3} $GdCl_3$, using different concentrations of APS as oxidant. It was found that the PANI particles are all about 80–200 nm as in Figures 2(a)–2(f). When the molar ratios of APS to aniline are 1 : 4 and 1 : 2, the PANI nanoparticles tend to agglomerate together, and with increasing the APS concentration, the PANI tend to form fiber-shaped morphology. When the molar ratio of APS to aniline is 2 : 1, PANI nanoparticles form and become more distinct. With further increase in APS content, the average size of PANI nanoparticles decreases to about 80 nm [see Figs. 2(e) and 2f)]. However, as a result of too much APS, PANI was peroxidized and the conductivity of PANI that is prepared is smaller than that of the others. Moreover, when the products were filtered, washed successively with 1.0 mol dm^{-3} HCl and ethanol, we found they can almost completely dissolve in ethanol. This may be due to the peroxidation of PANI so as to form some soluble small molecules. So, when the molar ratios of APS to aniline are between 1 : 1 and 2 : 1, the conditions are more desirable.

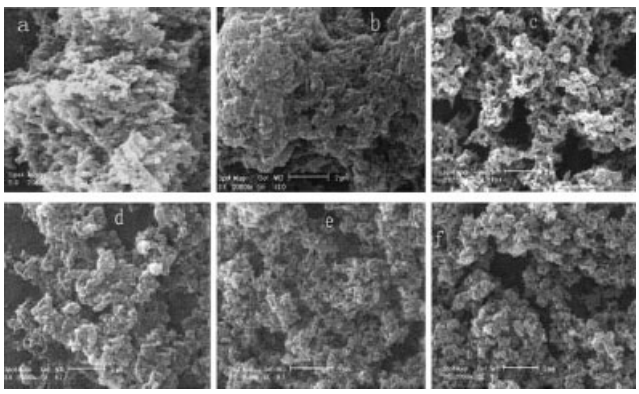

Figure 2 Effect of different proportions of APS on the morphology of PANI. The molar ratio of APS to aniline: (a) 1 : 4, (b) 1 : 2, (c) 1 : 1, (d) 2 : 1, (e) 4 : 1, and (f) 6 : 1.

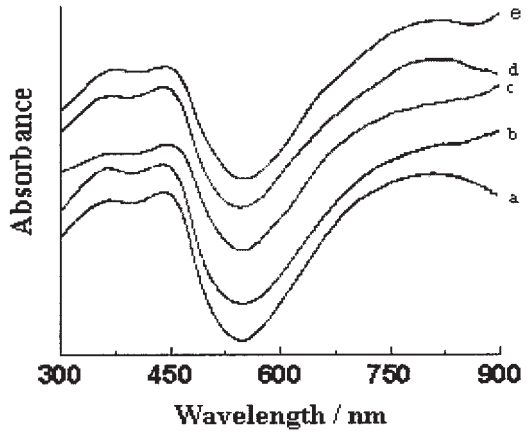

Figure 3 UV-vis spectra of PANI prepared at different concentrations of $GdCl_3$ (a) 0.2 mol dm^{-3} aniline + 1.0 mol dm^{-3} HCl, (b) 0.2 mol dm^{-3} aniline + 1.0 mol dm^{-3} HCl + 0.08 mol dm^{-3} $GdCl_3$, (c) 0.2 mol dm^{-3} aniline + 1.0 mol dm^{-3} HCl + 0.2 mol dm^{-3} $GdCl_3$, (d) 0.2 mol dm^{-3} aniline + 1.0 mol dm^{-3} HCl + 0.4 mol dm^{-3} $GdCl_3$, and (e) 0.2 mol dm^{-3} aniline + 1.0 mol dm^{-3} HCl + 0.8 mol dm^{-3} $GdCl_3$.

UV–vis spectra of PANI films

Figure 3 shows the UV–vis absorption spectra of resulting products, which were prepared in the solution containing 1.0 mol dm^{-3} HCl, 0.2 mol dm^{-3} aniline, and different concentrations of $GdCl_3$, using 0.2 mol dm^{-3} APS as oxidant. The characteristic peaks of control HCl-doped PANI appear at 368 nm due to π–π^* transition of the benzenoid ring and at 440 and 853 nm due to polaron–π^* and π–polaron band transitions,[30,31] respectively. This suggests that the earlier-mentioned PANI are in the doped state. It is interesting to note that the corresponding spectrum bands due to π–π^* and π–polaron transitions of PANI exhibit blue-shift with increasing concentration of $GdCl_3$ in the solution compared with that of PANI doped only by protonic acids (curve a), and the peaks at about 440 nm due to polaron–π^* transitions hardly change. With increasing $GdCl_3$ concentration, the peaks due to π–π^* and π–polaron transitions shift to around 360 and 845 nm. These results indicate that there exists interaction between Gd^{3+} and PANI chain,[29] which makes the energy transitions for π–π^* and π–polaron larger. In addition, the higher concentration of $GdCl_3$ improves the doping degree of PANI and promotes the diffusion of Gd^{3+} into the PANI chain, leading to increase in the coordination of Gd^{3+} with PANI chain. So, it is understandable that the absorption peaks shift to the shorter wavelength with increasing $GdCl_3$ concentration. However, with further increase of $GdCl_3$ concentration in the solution, the peak due to π–π^* transition of the benzenoid ring tends to come back to that of PANI prepared without $GdCl_3$; again, this may be because there exists an optimum in the effective conjugation length with the increasing of $GdCl_3$ concentration.[32]

Figure 4 shows the UV–vis absorption spectra of PANI prepared in the solution containing 1.0 mol dm^{-3} HCl, 0.2 mol dm^{-3} aniline, and 0.4 mol dm^{-3} $GdCl_3$, using different concentrations of APS as oxidant. The samples (a–d) present basically three characteristic absorption bands at about 360, 430, and 850 nm, as described in Figure 4, which shows that the above-mentioned PANI are in the doped state. With the increase in APS content, the corresponding bands tend to shift to the longer wavelength. This is because the optimum amount of APS made the conjugation chain enlarged, which made the energy for π–π^* and π–polaron transitions smaller. However, when the molar ratio of APS to aniline is 4 : 1, due to the strong oxidative ability of excessive APS, PANI was peroxidized and the characteristic absorption peaks of the UV–vis absorption spectra almost disappeared (curve e in Fig. 4).

FTIR spectra of PANI powder

Figure 5 shows the FTIR spectra of resulting products, which were prepared in 1.0 mol dm^{-3} HCl solution containing 0.4 mol dm^{-3} aniline and different concentrations of $GdCl_3$, using 0.2 mol dm^{-3} APS as oxidant. It was found that the FTIR spectra of these PANI prepared are similar to each other, which indicates that the backbone structures of PANI are identical to each other. The characteristic peaks at about 1556 and 1477 cm^{-1} are assigned to the stretching vibrations of N═Q═N ring, N—B—N ring, respectively (where B refers to the benzenic-type rings and Q refers to the quinonic-type rings). The peak at 1293 cm^{-1} corresponds to C—N stretching vibration. The peaks at 1111 and 796 cm^{-1} are attributed to the characteristics of B—NH—Q or B—NH—B bonds, and out-of-plane bending vibration of C—H on the 1,4-disubstituted, respectively. The PANI spectrums present a good

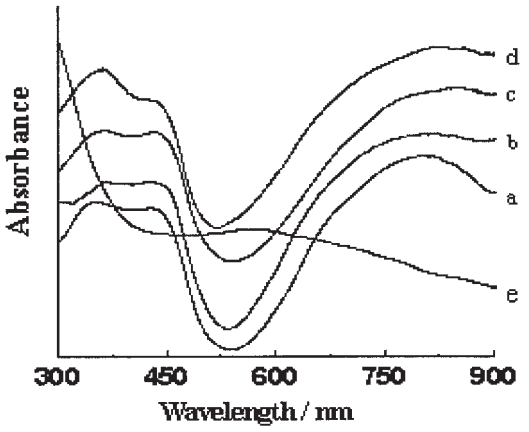

Figure 4 Effect of different proportions of APS on the UV-vis spectra of PANI/Gd^{3+}, the molar ratio of APS to aniline: (a) 1 : 4, (b) 1 : 2, (c) 1 : 1, (d) 2 : 1, and (e) 4 : 1.

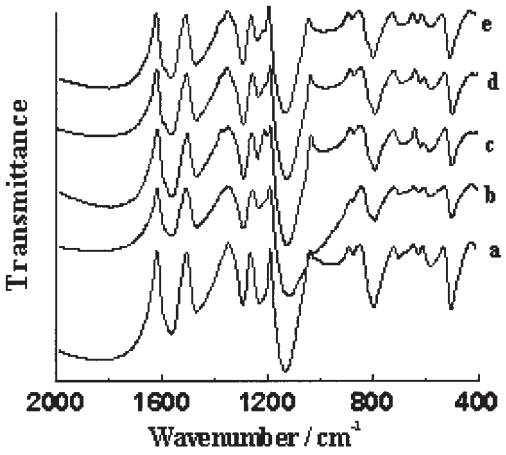

Figure 5 FTIR spectra of PANI prepared at different concentrations of $GdCl_3$ (a) 0.2 mol dm^{-3} aniline + 1.0 mol dm^{-3} HCl, (b) 0.2 mol dm^{-3} aniline + 1.0 mol dm^{-3} HCl + 0.08 mol dm^{-3} $GdCl_3$, (c) 0.2 mol dm^{-3} aniline + 1.0 mol dm^{-3} HCl + 0.2 mol dm^{-3} $GdCl_3$, (d) 0.2 mol dm^{-3} aniline + 1.0 mol dm^{-3} HCl + 0.4 mol dm^{-3} $GdCl_3$, and (e) 0.2 mol dm^{-3} aniline + 1.0 mol dm^{-3} HCl + 0.8 mol dm^{-3} $GdCl_3$.

agreement with the literature,[33] except for a few shifts in the wavenumbers.

When PANI was obtained in the solution containing 0.08 mol dm^{-3} of $GdCl_3$, the peaks of the quinoid units shifted to higher wavenumbers compared with that of PANI obtained without $GdCl_3$ (curve a in Fig. 5). The band at 1556 cm^{-1} due to C═C stretching vibrations of quinoid units shift to 1558 cm^{-1}, and the peak at 1111 cm^{-1} owing to the in-plane C—H bending modes of quinoid ring shifts to 1122 cm^{-1}; other peaks are almost not shifted. When the concentration of $GdCl_3$ is 0.2 mol dm^{-3}, these two characteristic bands shift to 1561 and 1122 cm^{-1}, respectively. The facts indicate that there exists interaction between the paramagnetic ion Gd^{3+} and PANI chain, and the Gd^{3+} may coordinate with imine nitrogen atoms in PANI chain,[10,34] which leads to the higher energy for the bands of quinoid units comparing with that of PANI-HCl (curve a in Fig. 5). The results are in agreement with the conclusion drawn from UV–vis spectra. However, with further increase in $GdCl_3$ concentration, the corresponding peaks come back to that of PANI prepared without $GdCl_3$; again, the reason is similar to that of the earlier mentioned.

Figure 6 shows the FTIR spectra of PANI prepared in 1.0 mol dm^{-3} HCl solution containing 0.2 mol dm^{-3} aniline, 0.4 mol dm^{-3} $GdCl_3$, and different concentrations of APS. It was found that the FTIR spectra of these PANI prepared are similar to each other, except for a few shifts in the wavenumbers. This fact indicates that the backbone structures of PANI obtained are identical to each other. When the molar ratio of APS to aniline is 1 : 4, the main characteristic peaks appear at 1548, 1476, 1292, 1140, and 793 cm^{-1}. When the content of APS is increased, the peak at 1140 cm^{-1} owing to the in-plane C—H bending modes of quinoid ring shifts to 1112 cm^{-1} and other peaks are almost not shifted; furthermore, the peaks become stronger. This is because the optimum amount of APS improved the degree of polymerization of aniline and enhanced the length of conjugation, which makes the energy for the in-plane C—H bending modes of quinoid ring lesser. In addition, when the molar ratios of APS to aniline are 1 : 4 and 1 : 2, a strong peaks appear at 1014 and 1008 cm^{-1}, respectively. According to the literature,[35] in the region of 1010–1170 cm^{-1}, the aromatic C—H in-plane bending modes are usually observed. When the molar ratios of APS to aniline are 4 : 1 and 6 : 1, new peaks appear at 1375 and 1383 cm^{-1}, respectively. The bands at 1375 and 1383 cm^{-1} are attributed to the stretching modes of a C—N bond of the aromatic amine, which exists in different chemical environments.[36] However, when too much of APS was added into the solution, the corresponding peaks shift to higher wavenumbers. When the molar ratio of APS to aniline is 4 : 1, the main characteristic peaks appear at 1578, 1497, 1303, 1141, and 802 cm^{-1}. When the content of APS is too high in the solution, PANI was peroxidized, which results in shifting to higher wavenumbers.

XRD analysis

Figure 7 shows the XRD patterns of the PANI-HCl and PANI/Gd^{3+} powder. The PANI-HCl powder exhibits a broad amorphous reflection at $2\theta \cong 25°$, whereas the samples of PANI/Gd^{3+} have several stronger diffraction peaks. The presence of peaks between 2θ-values of 8° and 30° in the samples reveals the local crystalline nature of the PANI/Gd^{3+}.[37–39] Two peaks centered at $2\theta \cong 22°$ and 25° were observed in X-ray scattering patterns of all PANI salts. The peak of $2\theta \cong 9°$ is assigned to the scattering along the orientation

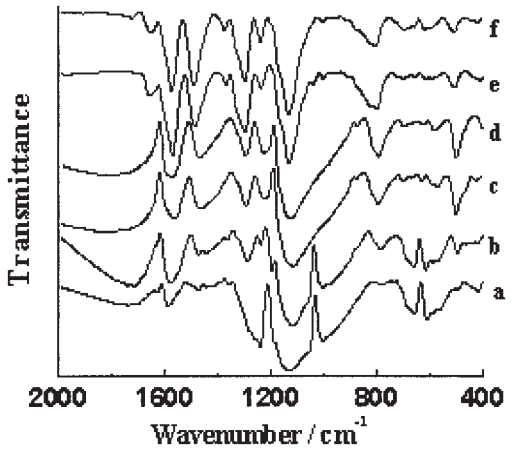

Figure 6 Effect of different proportions of APS on the FTIR spectra of PANI/Gd^{3+}, the molar ratio of APS to aniline: (a) 1 : 4, (b) 1 : 2, (c) 1 : 1, (d) 2 : 1, (e) 4 : 1, and (f) 6 : 1.

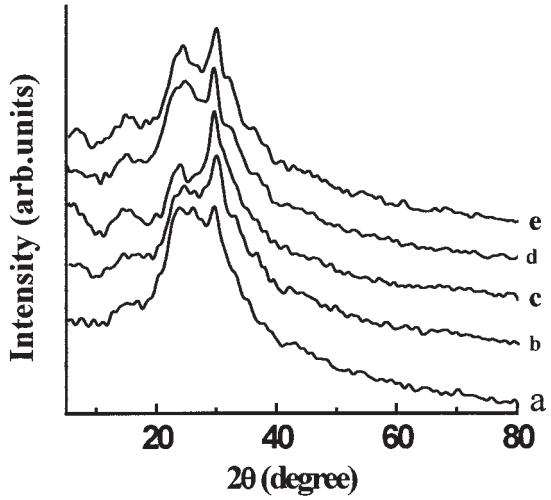

Figure 7 The X-ray diffraction spectra of PANI prepared at different concentrations of $GdCl_3$:(a) 0.2 mol dm^{-3} aniline + 1.0 mol dm^{-3} HCl (b) 0.2 mol dm^{-3} aniline + 1.0 mol dm^{-3} HCl + 0.08 mol dm^{-3} $GdCl_3$, (c) 0.2 mol dm^{-3} aniline + 1.0 mol dm^{-3} HCl + 0.2 mol dm^{-3} $GdCl_3$, (d) 0.2 mol dm^{-3} aniline + 1.0 mol dm^{-3} HCl + 0.4 mol dm^{-3} $GdCl_3$, and (e) 0.2 mol dm^{-3} aniline + 1.0 mol dm^{-3} HCl + 0.8 mol dm^{-3} $GdCl_3$.

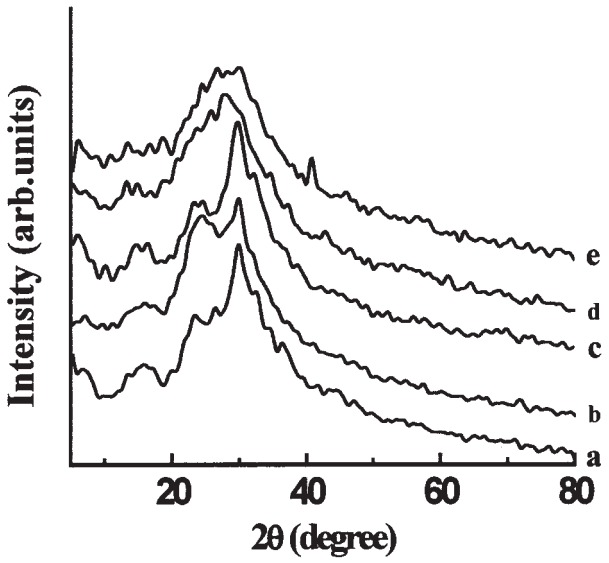

Figure 8 Effect of different proportions of APS on the X-ray diffraction patterns of PANI/Gd^{3+}, the molar ratio of APS to aniline: (a) 1 : 4, (b) 1 : 1, (c) 2 : 1, (d) 4 : 1, and (e) 6 : 1.

parallel to the PANI chain and the peak centered at $2\theta \cong 22°$ may be ascribed to periodicity parallel to the polymer chain, while the peaks at $2\theta \cong 25°$ may be caused by the periodicity perpendicular to the polymer chain.[40] The peak at $2\theta \cong 22°$ also represents the characteristic distance between the ring planes of benzene rings in adjacent chains or the close-contact interchain distance.[41] These results indicate that the PANI subchains become more rigid and ordered under the influence of Gd^{3+} and the degree of crystallinity is higher for PANI/Gd^{3+} than that of PANI-HCl. This higher crystallographic order of the polymer chains causes a decreased separation of the chains and increased conductivity. In addition, it is known that PANI of high crystallinity has a higher conductivity than amorphous one,[42] so, it is understandable that the conductivity of PANI/Gd^{3+} powder is higher than that of PANI-HCl.

Figure 8 shows the XRD patterns of PANI prepared in the solution containing 1.0 mol dm^{-3} HCl, 0.2 mol dm^{-3} aniline, 0.4 mol dm^{-3} $GdCl_3$, and different concentrations of APS. The curves a–c in Figure 8 are similar to each other; but when the molar ratio of APS to aniline is 1 : 1 and 2 : 1, the diffraction peaks appear at $2\theta \cong 22°$ and are stronger than that of PANI prepared when the molar ratios of APS to aniline are 4 : 1 and 6 : 1. It was concluded from these facts that the PANI prepared is the local crystalline nature, and in the special range, the effects of APS content on the degree of crystallinity are not much; their similar conductivity also proved this. However, when the molar ratios of APS to aniline are 4 : 1 and 6 : 1, the PANI powder exhibits a broad amorphous reflection at $2\theta \cong 25°$, and the conductivity of these two PANI samples is about 3–4 order of magnitude smaller than that of the others; the reasons have been mentioned earlier.

Differential thermal analysis

Figure 9 shows the DTA curves of PANI-HCl and PANI/Gd^{3+} powder, which were prepared in the so-

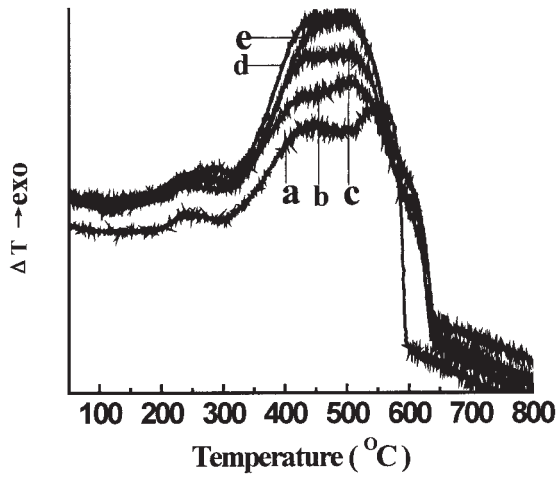

Figure 9 The DTA patterns of PANI prepared at different concentrations of $GdCl_3$ (a) 0.2 mol dm^{-3} aniline + 1.0 mol dm^{-3} HCl (b) 0.2 mol dm^{-3} aniline + 1.0 mol dm^{-3} HCl + 0.08 mol dm^{-3} $GdCl_3$, (c) 0.2 mol dm^{-3} aniline + 1.0 mol dm^{-3} HCl + 0.2 mol dm^{-3} $GdCl_3$, (d) 0.2 mol dm^{-3} aniline + 1.0 mol dm^{-3} HCl+ 0.4 mol dm^{-3} $GdCl_3$, and (e) 0.2 mol dm^{-3} aniline + 1.0 mol dm^{-3}HCl + 0.8 mol dm^{-3} $GdCl_3$. Heating rate: 10°C min^{-1}, from 50 to 800°C.

lution containing 1.0 mol dm^{-3} HCl, 0.2 mol dm^{-3} aniline, and different concentrations of $GdCl_3$, using 0.2 mol dm^{-3} APS as oxidant. It was found from Figure 9 that all samples exhibit a similar thermal behavior, with a small variation in degradation temperature. Thermal effects at destruction of PANI-HCl (Fig. 9 curve a) involve the volatilization and decomposition of water and other small molecules or oligomer units at the first stage of destruction (endopeak at 150°C) and considerable exo-effects of structure transformation in the temperature range 190–500°C, which is consistent with the literature.[43] As temperature increases further, a gradual decrease in heat content as a result of the carbonization processes is observed. Other way, these processes are accompanied by a decrease in heat capacity, which is a typical feature for those processes in organic nitrogen-containing polymers.[44,45] As for the samples of PANI/Gd^{3+}, the thermal destruction characteristics are similar to those of PANI-HCl, except for a few shifts in the temperature range, as shown in Table II. With the increase in $GdCl_3$ content, the temperature range of peaks that was assigned to the elimination of dopant ions in the polymers decreases, which indicates that the added Gd^{3+} can dope into PANI chain and they may coordinate with nitrogen atoms in PANI chains. This coordination effect weakens the strength of N—H bond on PANI chains resulting in the more easiness to the loss of HCl dopant for PANI/Gd^{3+}.

Figure 10 shows the DTA patterns of PANI prepared in 1.0 mol dm^{-3} HCl solution containing 0.2 mol dm^{-3} aniline, 0.4 mol dm^{-3} $GdCl_3$, and different concentrations of APS. The curves b and c in Figure 10 are similar to that of Figure 9. With increasing APS content, the temperature ranges that were assigned to the decomposition of some existing monomer and oligomer units and exo-effects of structure transformation increase. Moreover, the single peaks in curves d and e suggest the lower doping degree due to the peroxidation of PANI. DTA analysis (Fig. 10, curve e)

TABLE II
Thermal Parameters of Polymers

	Range of temperature (°C)		
	Range 1	Range 2	Range 3
Sample (Fig. 9)			
(a)	50–160	190–445	550–590
(b)	50–160	190–435	510–635
(c)	50–120	160–435	510–640
(d)	50–120	150–430	500–645
(e)	50–120	145–430	495–640
Sample (Fig. 10)			
(a)	50	100	520
(b)	50	140	510
(a)	50	140	510
(d)	50	160	510

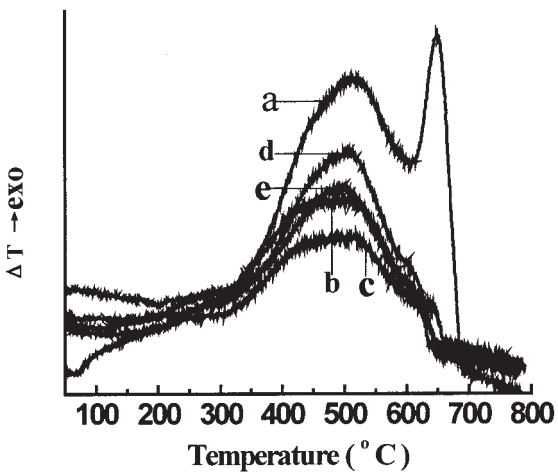

Figure 10 Effect of different proportions of APS on DTA patterns of PANI/Gd^{3+}, the molar ratio of APS to aniline: (a) 1 : 4, (b) 1 : 2, (c) 2 : 1, (d) 4 : 1, and (e) 6 : 1. Heating rate: 10°C min^{-1}, from 50 to 800°C.

shows the melting of sample with a pronounced endothermic effect at 200°C. The strong peak in curve a (at about 650°C) may be due to the decomposition of aniline–$GdCl_3$ coordination; however, more studies are needed to clarify the phenomenon.

CONCLUSIONS

In summary, the addition of $GdCl_3$ has effects on properties of chemically synthesized PANI. Comparing with that of PANI-HCl, the suitable concentrations of $GdCl_3$ lead to the bands of C═C stretching vibrations, and in-plane C—H bending modes of quinoid units shift to higher wavenumbers, and the energy for quinoid ring transition of $GdCl_3$-doped PANI in UV–vis spectra increases, which show that there exists interaction between Gd^{3+} and PANI chains. The conductivity and the degree of crystallinity are greatly increased under the influence of $GdCl_3$. Furthermore, when the concentration of Gd^{3+} is 0.2–0.4 mol dm^{-3}, the conductivity and degree of crystallinity are higher and the SEM morphology is more distinct and uniform.

This work also studied the effect of APS content in the presence of Gd^{3+}. As for the PANI synthesized chemically, when the molar ratios of APS as aniline are 1 : 1 and 2 : 1, the conductivity and degree of crystallinity are higher. With further increasing of APS content, the conductivity decreases rapidly, which is about 3–4 order of magnitude smaller than that of the PANI obtained with desirable content APS. When the content of APS is too high in the solution, PANI was peroxidized and the thermal degradation temperature of PANI backbone chains also decreased.

References

1. Gustafsson, G.; Cao, Y.; Treacy, G. M.; Klavetter, F.; Colaneri, N.; Heeger, A. J. Nature 1992, 357, 477.

2. MacDiarmid, A. G. Synth Met 1997, 84, 27.
3. Martin, C. R. Science 1994, 266, 1961.
4. Galloppa, A.; Cataldo, F.; Campoli, F.; Maltese, P. Mol Cryst Liq Cryst 1996, 290, 129.
5. Li, W.; Xie, S.; Qian, L.; Chang, B.; Zou, B.; Zhou, W.; Zhao, R.; Wang, G. Science 1996, 274, 1701.
6. Sakai, H.; Baba, R.; Hashimoto, K.; Fujishima, A.; Heller, A. J Phys Chem 1995, 99, 11896.
7. Trau, M.; Yao, N.; Kim, E.; Xia, Y.; Whitesides, G. M.; Aksay, I. A. Nature 1997, 390, 674.
8. Gardnera, J. W.; Bartlett, P. N. Sens Actuators A 1995, 51, 57.
9. Kan, J.; Pan, X.; Chen, C. Biosens Bioelectron 2004, 19, 1635.
10. Dimitriev, O. P.; Kislyuk, V. V. Synth Met 2002, 132, 87.
11. Hasik, M.; Drelinkiewicz, A.; Wenda, E. Synth Met 2001, 119, 335.
12. MacDiarmid, A. G.; Epstein, A. J. Faraday Discuss Chem Soc 1989, 88, 317.
13. Huang, S.; Neoh, K. G.; Kang, E. T.; Han, H. S.; Tan, K. L. J Mater Chem 1998, 8, 1743.
14. Zeng, X. B.; Zhang, Y. F.; Shen, Z. Q. J Polym Sci Part A: Polym Chem 1997, 35, 2177.
15. Cai, L.; Yao, S.; Zhou, S. Synth Met 1997, 88, 205.
16. Shipley, C. P.; Salata, O. V.; Capecchi, S.; Christou, V.; Dobson, P. J Adv Mater 1999, 11, 533.
17. Lin, Q.; Shi, C. Y.; Liang, Y. Y. J.; Zheng, Y. X.; Wang, S. B.; Zhang, H. J. Synth Met 2000, 114, 373.
18. Kobayashi, N.; Uemura, S.; Kusabuka, K.; Nakahira, T.; Takahashi, H. J Mater Chem 2001, 11, 1766.
19. Wu, C. G.; Hsiao, H. T.; Yeh, Y. R. J Mater Chem 2001, 11, 2287.
20. Cazeca, M. J.; Chittibabu, K. G.; Kim, J.; Kumar, J.; Jain, A.; Kim, W.; Tripathy, S. K. Synth Met 1998, 98, 45.
21. Male, N. A. H.; Salata, O. V.; Christou, V. Synth Met 2002, 126, 7.
22. Hirao, T.; Higuchi, M.; Hatano, B.; Ikeda, I. Tetrahedron Lett 1995, 36, 5925.
23. Kumaki, J. Macromolecules 1986, 19, 2258.
24. Henselwood, F.; Liu, G. Macromolecules 1997, 30, 488.
25. Erdem, E.; Karakisla, M.; Sacak, M. Eur Polym J 2004, 40, 785.
26. Stupp, I. Sci News 1986, 129, 297.
27. Wang, Y.; Zhang, X.; Liu, X.; Su, X. Chin J Power Sources 2004, 28, 231.
28. Kan, J.; Mu, S. Acta Polym Sin 1989, 4, 466.
29. Forsberg, J. H. Coord Chem Rev 1973, 10, 195.
30. Lu, F. L.; Wudl, F.; Nowak, M.; Heeger, A. J. J Am Chem Soc 1986, 108, 8311.
31. Stafstrom, S.; Breadas, J. L.; Epstein, A. J.; Woo, H. S.; Tenner, D. B.; Huang, W. S.; Macdiarmid, A. G. Phys Rev Lett 1987, 59, 1464.
32. Yin, W.; Ruckenstein, E. Synth Met 2000, 108, 39.
33. Zeng, X.; Ko, T. J Polym Sci 1997, 35, 1993.
34. Dimitriev, O. P. Polym Bull 2003, 50, 83.
35. Trchova, M.; Sedenkova, I.; Tobolkova, E.; Stejskal, J. Polym Degrad Stab 2004, 86, 179.
36. Cao, Y.; Li, S.; Xue, Z.; Guo, D. Synth Met 1986, 16, 305.
37. Svetlicic, V.; Schmidt, A. J.; Miller, L. L. Chem Mater 1998, 10, 3305.
38. Joo, J.; Chung, Y. C.; Song, H. G.; Baeck, J. S.; Lee, W. P.; Epstein, A. J.; MacDiarmid, A. G. Synth Met 1997, 84, 739.
39. Pouget, J. P.; Jozefowicz, M. E.; Epstein, A. J.; Tang, X.; MacDiarmid, A. G. Macromolecules 1991, 24, 779.
40. Moon, Y. B.; Cao, Y.; Smith, P.; Heeger, A. J. Polym Commun 1989, 30, 196.
41. Pouget, J. P.; Hsu, C. H.; MacDiarmid, A. G.; Epstein, A. J. Synth Met 1995, 69, 119.
42. Kim, B. J.; Oh, S. G.; Han, M. G.; Im, S. S. Synth Met 2001, 122, 297.
43. Elyashevich, G. K.; Terlemezyan, L.; Kuryndin, I. S.; Lavrentyev, V. K.; Mokreva, P.; Rosova, E. Y.; Sazanov, Y. N. Thermochim Acta 2001, 374, 23.
44. Sazanov, Y. N. Thermal Analysis of Organic Compounds; Nauka: Moscow, 1991, p 141 (in Russian).
45. Yang, C. M.; Fang, Z.; Liu, J. B.; Liu, W. P.; Zhou, H. Thermochim Acta 2000, 352, 159.